

The dynamic influence of methane seepage on macrofauna inhabiting authigenic carbonates

OLÍVIA S. PEREIRA ^{1,†}, JENNIFER GONZALEZ,¹ GUILLERMO F. MENDOZA,¹ JENNIFER LE,¹ CONNOR L. COSCINO,¹ RAYMOND W. LEE,² JORGE CORTÉS,³ ERIK E. CORDES ⁴, AND LISA A. LEVIN ¹

¹*Integrative Oceanography Division and Center for Marine Biodiversity and Conservation, Scripps Institution of Oceanography, University of California San Diego, San Diego, California, USA*

²*School of Biological Sciences, Washington State University, Pullman, Washington, USA*

³*Centro de Investigación en Ciencias del Mar y Limnología, Universidad de Costa Rica, San José, Costa Rica*

⁴*Department of Biology, Temple University, Philadelphia, Pennsylvania, USA*

Citation: Pereira, O. S., J. Gonzalez, G. F. Mendoza, J. Le, C. L. Coscino, R. W. Lee, J. Cortés, E. E. Cordes, and L. A. Levin. 2021. The dynamic influence of methane seepage on macrofauna inhabiting authigenic carbonates. *Ecosphere* 12(10):e03744. 10.1002/ecs2.3744

Abstract. Methane seeps are highly productive deep-sea ecosystems reliant on chemosynthetic primary production. They are increasingly affected by direct human activities that threaten key ecosystem services. Methane seepage often generates precipitation of authigenic carbonate rocks, which host diverse microbes, and a dynamic invertebrate community. By providing hard substrate, even after seepage ceases, these rocks may promote a long-lasting ecological interaction between seep and background communities. We analyzed community composition, density, and trophic structure of invertebrates on authigenic carbonates at Mound 12, a seep on the Pacific margin of Costa Rica, using one mensurative and two manipulative experiments. We asked whether carbonate macrofaunal communities are able to survive, adapt, and recover from changes in environmental factors (i.e., seepage activity, chemosynthetic production, and food availability), and we hypothesized a key role for seepage activity in defining these communities and responses. Communities on *in situ* carbonates under different seepage activities showed declining density with increasing distance from the seep and a shift in composition from gastropod dominance in areas of active seepage to more annelids and peracarid crustaceans that are less dependent on chemosynthetic production under lesser seepage. Response to changing environmental context was evident from altered community composition following (1) a natural decline in seepage over successive years, (2) transplanting of carbonates to different seepage conditions for 17 months, and (3) defaunated carbonate deployments under different seepage regimes over 7.4 yr. Seep faunas on transplants to lesser seepage emerge and recover faster than transition fauna (characterized by native seep and background faunas, respectively) and are able to persist by adapting their diets or by retaining their symbiotic bacteria. The macrofaunal community colonizing defaunated carbonates deployed for 7.4 yr developed communities with a similar successional stage as *in situ* rocks, although trophic structure was not fully recovered. Thus, macrofaunal successional dynamics are affected by habitat complexity and the availability of microbial chemosynthetic productivity. This multi-experiment study highlights the interaction between biotic and abiotic factors at methane seeps at different time scales along a spatial gradient connecting seep and surrounding deep-sea communities and offers insight on the resilience of deep-sea macrofaunal communities.

Key words: authigenic carbonates; community composition; community dynamics; community resilience; invertebrate macrofauna; methane seep; trophic structure.

Received 15 December 2020; revised 16 April 2021; accepted 23 April 2021. Corresponding Editor: Hunter S. Lenihan.

Copyright: © 2021 The Authors. This is an open access article under the terms of the Creative Commons Attribution License, which permits use, distribution and reproduction in any medium, provided the original work is properly cited.

† **E-mail:** ospereir@ucsd.edu

INTRODUCTION

The deep ocean hosts extreme environments that support unique communities reliant on chemosynthesis rather than photosynthesis (Tunnicliffe et al. 2003); they are highly productive due to microbial energy capture from the oxidation of sulfide, methane, and hydrogen (Dubilier et al. 2008). Among these systems, methane seeps play key roles in climate regulation and carbon sequestration through aerobic and anaerobic methane oxidation (AOM) and carbonate precipitation (regulating services; Boetius and Wenzhofer 2013, Marlow et al. 2014b). Seeps are often associated with hydrocarbon resources (Boetius and Wenzhofer 2013) and also provide supporting (or intermediate) services through interaction with background fish and invertebrate faunas and cultural services such as education (Grupe et al. 2015, Levin et al. 2016). Methane seeps have been found to sustain commercially important species, such as tanner and red crabs, that use the seeps for trophic and reproductive support (Seabrook et al. 2019, Turner et al. 2020). The Pacific Fishery Management Council recently recognized methane seeps and associated biota as essential fish habitat in the world's first incorporation of seeps in fisheries management (NOAA 2020).

Seeps are found globally on both active and passive continental margins (Ritt et al. 2010) from continental shelf and slope depths (>22 m) (Paul et al. 2017) to trenches (up to 7326 m) (Fujikura et al. 1999). Precipitation of carbonate rocks at methane seeps is a by-product of the anaerobic oxidation of methane (AOM) (Bahr et al. 2009) carried out by aggregates of anaerobic methane oxidizing archaea (ANMEs) and sulfate-reducing gamma-proteobacteria (SRBs) in the sediment (Boetius et al. 2000, Orphan et al. 2002, Reeburg 2007). Thus, although much of the deep ocean is covered by sediments, seeps are frequently associated with extensive cover of authigenic carbonates (Aloisi et al. 2000).

Seepage activity is dynamic, sensitive to tectonics in the long term (Mau et al. 2007), and to tides (Tryon et al. 1999), disturbance of sediments, oxygen availability, and microbial activity in the short term (Linke et al. 2005). Understanding the natural dynamics that affect the

environmental context and ecological interactions at seeps is important for effective spatial planning, resource management, valuation, and conservation, given their vulnerability to disturbance from intensifying resource extraction and waste disposal on margins (Ramirez-Llodra et al. 2011, Mengerink et al. 2014). Previous studies at seeps have shown that the associated communities vary on different time scales. Microbial communities are able to adapt to changing environmental conditions and methane fluxes on the scale of hours to days (Marlow et al. 2014b, Case et al. 2015). The megabenthic fauna go through successional processes on the scale of years to decades (Cordes et al. 2005) but can also be significantly influenced by season (Doya et al. 2017) and tidal periodicity (Girard et al. 2020).

The habitat heterogeneity introduced by carbonates substantially contributes to the diversity of seep macrofauna, which uses hard substrata for attachment, shelter, and access to food (Levin et al. 2015, 2017). When seepage activity ceases, the carbonates remain, attracting background species that feed on remaining debris or use the structures to gain access to particles in the water (Bowden et al. 2013). Thereby, carbonates promote an interaction between native seep and background communities that may last for centuries (Levin et al. 2009, 2016). Exchange of organic material, energy, and nutrients between the seep and its surroundings through horizontal advection and by mobile predators and scavengers enhance ecosystem complexity (Levin et al. 2016), forming transition zones that have a mixture of native seep and non-seep species (Cordes et al. 2009, Ashford et al. 2021) and provide complex trophic interactions.

Trophic linkages are critical to ecosystem functioning as they transfer energy throughout food webs. Trophic pathways can be identified through stable isotope (usually $\delta^{13}\text{C}$ and $\delta^{15}\text{N}$) analyses as seeps exhibit large ranges of stable isotope ratios (Levin and Michener 2002, Thurber et al. 2012, Thurber 2014). ANME consortia typically have $\delta^{13}\text{C}$ values of -30‰ to -100‰ for archaeal cells and -15‰ to -70‰ for associated symbiotic SRB (Orphan et al. 2002, House et al. 2009), much more negative than typical products of photosynthesis (-15‰ to -25‰). These distinct isotopic compositions provide an ecological

means to explore trophic interactions (Thurber et al. 2012).

Previous research has documented macrofauna on authigenic carbonate rocks at Costa Rica seeps (Levin et al. 2015), and Hydrate Ridge, Oregon (Levin et al. 2017), and their colonization over 10.5 months (Grupe 2014). The overarching objectives of this work are to examine the dynamics of carbonate macroinvertebrates (< 300 μm), their trophic structure and to identify the relevant temporal and spatial scales of their response to changes in environmental context (i.e., seepage activity, chemosynthetic production, habitat heterogeneity and complexity, and food availability). These are examined by combining natural gradients and interannual variation in seepage with colonization and transplant experiments at a single site at different temporal scales (days to 7.4 yr). We ask if there is interannual variability in seepage community and trophic structure due to natural changes in environmental conditions, and we hypothesize that changing exposure to seepage affects native seep and background invertebrate macrofaunal communities on hard substrates differently, with higher resistance (persistence) by seep faunas and more resilience (rapid recolonization) by background fauna. We evaluate whether macrofauna colonizing defaunated carbonates fully recover natural patterns of community composition and trophic structure within 7.4 yr and hypothesize that recolonization varies with seepage activity. Finally, we discuss the implications of observed environmental interactions and successional dynamics for the vulnerability of seep communities to disturbance, and how this might influence conservation and management.

METHODS

Study area description and experimental design

The Pacific coast of Costa Rica is an offshore convergent margin exhibiting subduction and erosion of continental material (Sahling et al. 2008). Fluid venting has long been documented in the area (McAdoo et al. 1996), and there is evidence for more than 100 seep sites along 580 km of the Costa Rica margin, characterized by chemosynthetic communities and authigenic carbonates (Sahling et al. 2008). Mound 12 (8°55.8' N, 84°18.7' W, Fig. 1) is located on the

Costa Rica Pacific margin at 990–1000 m water depth (Mau et al. 2006), just below the oxygen minimum zone (Levin et al. 2015). It is a carbonate mound approximately 1–1.6 km in diameter with the main active seepage area located southwest of the mound summit (Mau et al. 2006), and approximately 85.7% of its volume comprises authigenic carbonates (Klaucke et al. 2008). Slope sediments intercalated with mudflows indicate an alternation of seepage with low-activity phases on geological time scales (Niemann et al. 2013), while seepage rate, as measured by methane release over the mound, can vary on annual time scales (Mau et al. 2007).

Results presented here are based on samples collected at Mound 12 during two research cruises aboard the *R/V Atlantis* (AT37-13: May to June 2017, and AT42-03: October 2018) using the submersible *Alvin*. To examine community and trophic response to seepage gradients, intact authigenic carbonate rocks (*in situ*) were taken at sites with high and lower/transition seepage activity in 2017 (five active, four transition) and 2018 (six active, seven transition; Fig. 1, Appendix S1: Table S1). High activity level was defined visually by the presence of microbial mats, methane bubbles, or native seep megafauna, as previously done by Levin et al. (2015). Transition sites were defined as areas devoid of the seep megafauna or bacterial mats but having carbonates that were within ~550 m of an active seep. Background (non-seep) sites did not have carbonates. Carbonate rocks were placed into individual plexiglass containers within Delrin bioboxes on the *Alvin* basket or in an “elevator” (benthic lander deployed as a free vehicle over the side of the *R/V Atlantis*) to avoid cross contamination of samples during recovery. The collected rocks were also used as control samples for two experiments.

Transplant experiment (Fig. 1).—To address the roles of changing seepage in determining the rates and trajectory of community response, carbonate rocks were transplanted in 2017 (AT37-13) by *Alvin* (without return to the ship) from an original location on the seafloor to a location with lesser seepage from: (1) active to inner transition ($n = 6$), (2) active to outer transition ($n = 5$), (3) active to background ($n = 5$), (4) inner transition to outer transition ($n = 5$), (5) inner transition to background sites ($n = 5$), or

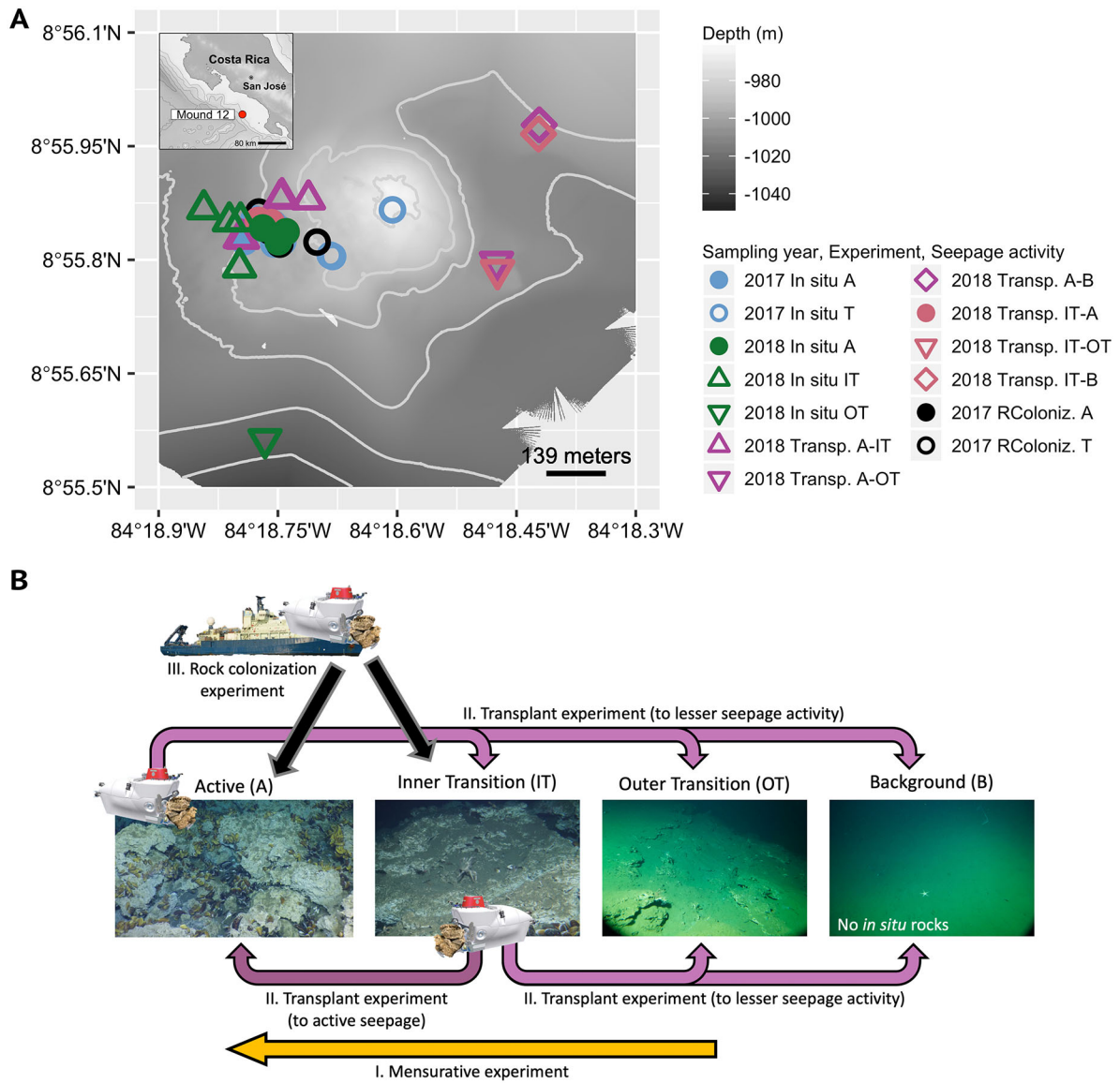


Fig. 1. Sampling locations of authigenic carbonate rocks at Mound 12, a seep site off the Pacific margin of Costa Rica, and experimental design. (A) Sampling locations for all experiments at all seepage activity sites. Marker colors reflects experiment: purple, *in situ* rocks collected in 2017; orange, *in situ* rocks collected in 2018; pink, rocks transplanted across seepage activity for 17 months (2017–2018; Transplant experiment—Transp.); blue, rocks deployed at active and transition sites for 7.4 yr (2010–2017; Rock colonization experiment—RColoniz.). Marker shapes reflect seepage activity at collection site: filled circle, active; open circle, transition; up-pointing triangle, inner transition; down-pointing triangle, outer transition; diamond, background. Seepage activity abbreviations: A: Active, T: Transition, IT: Inner transition, OT: Outer transition, B: Background. (B) Experimental design: (I) Sampling *in situ* rocks across seepage gradients (yellow arrow), (II) Transplant experiment to lesser seepage activity (light purple arrows) or to more active seepage (dark purple arrows), and (III) Rock colonization experiment (black arrows).

(6) inner transition to active ($n = 5$; Appendix S1: Table S1). These were recovered by *Alvin* in 2018 (AT42-03) after 17 months.

Rock colonization experiment (Fig. 1).—Carbonate rocks obtained with *Alvin* from the Costa Rica margin in February–March 2009 on *R/V Atlantis* (AT15-44) were defaunated and dried for 10 months then deployed by the ROV *Jason* at Mound 12 on January 8, and 10, 2010 (AT15-59). To test the colonization patterns and rates of macrofaunal communities, eight defaunated rocks were deployed in active ($n = 4$) and transition sites ($n = 4$; Appendix S1: Table S1); these were recovered by *Alvin* (as described above) in May 2017 (AT37-13), approximately 7.4 yr after deployment.

CTD casts were made over Mound 12 during AT37-13 (May 22nd, 2017, 8°55.827' N, 84°18.757' W) and AT42-03 (October 20th, 2018, 8°55.864' N, 84°18.616' W, and October 24th, 2018, 8°55.852' N, 84°18.757' W). Bottom temperature ranged from 4.79 to 4.91°C, salinity ranged from 34.56 to 34.58, and dissolved oxygen concentration ranged from 27.1 to 30.55 $\mu\text{mol/L}$. Surface (<5 m) and near bottom (<15 m above bottom) water samples were collected via Niskin bottles on a CTD Rosette for analysis of particulate organic carbon (POC) stable isotopic composition.

Shipboard processing

The associated fauna on the carbonate rocks and in the recovery container was removed from each rock/container upon recovery, sorted, and identified to lowest possible taxonomic level using a dissecting microscope. Following this, rocks were wrapped in aluminum foil to determine the approximate rock surface area later in the laboratory and then placed in filtered seawater and left at room temperature overnight to allow additional fauna within the rock crevices to crawl out. These were sieved on a 0.3 mm mesh and preserved in 95% ethanol to be sorted in the laboratory.

To examine their relative reliance on seep productivity and changes in trophic structure, tissue subsamples from three live specimens of each morpho-species were collected for stable isotope analyses (Levin and Mendoza 2007). The tissue subsamples were washed in milli-Q water, placed in pre-weighed tin capsules or glass vials (combusted at 500°C for 4 h) and frozen at -20°C .

To evaluate the carbon and nitrogen isotopic signatures of particulate organic carbon (POC), 2–4 L of bottom water from each CTD cast was filtered through a glass microfiber filter, and the filter was frozen at -20°C until processing for isotope analysis.

Laboratory processing

At Scripps Institution of Oceanography, the aluminum foil was weighed to estimate rock surface area using a top-loading balance to an accuracy of 0.01 mg. The total weight of the foil was divided by the average weight of a 1 cm^2 piece of foil to determine the approximate rock surface area in cm^2 to calculate densities.

Macrofauna collected from carbonates was sieved using a 0.3-mm mesh and sorted in freshwater at 12 \times magnification under a dissecting microscope. Subsequent molecular sequencing revealed that some taxa identified morphologically as single species were found to be cryptic species (G.W. Rouse, *personal communication*), so species-level IDs were deemed unreliable and individuals in the most common phyla, Annelida and Mollusca, are discussed at the family level. Crustaceans were identified at the order or infraorder level, cnidarians at the order level, and echinoderms at the class level. The least abundant groups, Nemertea, Platyhelminthes, and Pycnogonida, were identified to phylum. Counts of animals that were removed at sea upon recovery for genetic or isotopic analyses were added to the laboratory counts to obtain total counts.

Animal tissue subsamples collected for stable isotope analyses were oven-dried at 60°C overnight, weighed, and acidified with 1N phosphoric acid to remove inorganic carbon. $\delta^{13}\text{C}$ and $\delta^{15}\text{N}$ measurements were made on 0.2–1 mg dry-weight samples combusted using a Costech elemental analyzer coupled to a Micromass IsoPrime isotope ratio mass spectrometer (EA/IRMS) at Washington State University (WSU). The glass microfiber filters were also sent to WSU for stable isotope measurements of the POC. Precision for $\delta^{13}\text{C}$ and $\delta^{15}\text{N}$ analyses were ± 0.02 and $\pm 0.05\text{‰}$, respectively (standard deviation of 10 replicate organic standards). For each rock, macrofaunal average signatures were determined by averaging replicates within each species then averaging species values.

Data management and statistical analyses

Density of the total macrofaunal community and individual species were standardized to number of individuals per 200 cm², the surface area for an average-sized rock, as in Levin et al. (2015). Density data could not always be transformed to achieve normal distribution or homogeneity of variance, thus non-parametric tests were performed. Wilcoxon tests were performed to check for variability of densities between sites, years, and experiments for data sets with two factors. For data sets with more than two factors, Kruskal-Wallis tests followed by Dunn's tests using the Benjamini-Hochberg adjustment (Benjamini and Hochberg 1995) were performed instead.

Community composition (i.e., identities of the taxa present in the community) is presented for major taxa as percent composition and also density (number of individuals per 200 cm²). Community count data were standardized by the total number of individuals and fourth-root transformed prior to calculating Bray-Curtis dissimilarity matrices, or conducting two-way ANOSIM and two-way SIMPER analyses using Primer v.6 (Clarke and Gorley 2015).

Stable isotope statistical analyses of mean values and community metrics were performed using routines implemented in the R environment (R Core Team 2016). As not all of the stable isotope data sets showed normal distribution or homogeneous variance even after log transformation, non-parametric tests were performed. To check for variability of isotope composition between sites, year, and experiments, Wilcoxon tests were performed for the data sets with two factors, and Kruskal-Wallis test followed by Dunn's test using the Benjamini-Hochberg adjustment (Benjamini and Hochberg 1995) were performed for data sets with more than two factors.

Community-level isotope metrics were generated in R with the SIBER package (Jackson et al. 2011) using standard elliptical area (SEA) and standard elliptical area corrected for sample size (SEAc) to represent relative isotopic niche areas (trophic diversity) in bivariate $\delta^{13}\text{C}$ and $\delta^{15}\text{N}$ space. Trophic diversity was also calculated as $\delta^{13}\text{C}$ and $\delta^{15}\text{N}$ ranges and total hull areas (TA) (Layman et al. 2007).

RESULTS

Natural seepage gradients and interannual variability

Density (Fig. 2A).—In 2017, the average density of invertebrate macrofauna on *in situ* carbonate rocks was more than 4× higher at active (238 ± 67 ind./200 cm²) than at transition sites (58 ± 16 ind./200 cm²), but densities were not significantly different ($W = 17$, $P = 0.11$). In 2018, there were no significant differences in density along a seepage gradient (40 ± 20 ind./200 cm² at active sites, 80 ± 21 ind./200 cm² at inner transition sites, and 43 ± 9 ind./200 cm² at outer transition sites; $\chi^2_2 = 3.81$, $P = 0.15$). At active sites, average total macrofaunal density was not significantly different between years ($W = 26$, $P = 0.052$). However, limpet and snail densities at active sites were significantly lower (limpets: $W = 28$, $P = 0.02$, snails: $W = 27$, $P = 0.03$) in 2018 (limpets: 2 ± 1 ind./200 cm², snails: 7 ± 4 ind./200 cm²) than 2017 (limpets: 124 ± 48 ind./200 cm², snails: 87 ± 44 ind./200 cm²). At transition sites, average total densities were not significantly different between 2017 and 2018 ($\chi^2_2 = 3.12$, $P = 0.21$).

Community composition (Fig. 2D).—Community composition varied significantly across seepage activity groups (two-way ANOSIM, Global $R = 0.397$, $P = 0.001$). In 2017, active sites were dominated by gastropods (52.3% limpets and 37.0% snails). At transition sites, annelids were the dominant group (42.4%), followed by gastropods (15.1% limpets and 12.2% snails), echinoderms (11.9%) and peracarids (8.4%). The groups contributing to the dissimilarity between the communities at active and transition sites (SIMPER, average dissimilarity = 68.12) were Amphipoda, Tanaidacea, Ophiuroidea, Serpulidae, Chrysopetalidae, and Hydroidolina present mainly at transition sites (Table 1), and gastropods in the families Neolepetopsidae, Provanidae and Cataegidae, and Anomura that were more abundant at active sites (Table 1).

In 2018, there was a composition change along a seepage gradient from an annelid- and gastropod-dominated community (53.5% annelids and 22.9% gastropods) at active sites to an annelid-dominated community at inner transition sites (82.9%). Chrysopetalid, syllid, and maldanid polychaetes were the most abundant

Table 1. Top ten taxa given as percent of the total for each seepage activity, based on densities for *in situ* carbonate rocks collected in different seepage regimes at Mound 12 in 2017.

Taxa	Percentage
2017 Active	
Provannidae	30.16
Lepetodrilidae	25.53
Neolepetopsidae	22.14
Skeneidae	5.14
Pyropeltidae	3.94
Anomura	1.21
Nuculanidae	1.21
Ampharetidae	1.17
Hesionidae	1.13
Serpulidae	1.05
Top ten total	92.67
2017 Transition	
Serpulidae	17.53
Chrysopetalidae	9.74
Neolepetopsidae	9.74
Provannidae	7.79
Amphipoda	6.82
Ophiuroidea	6.82
Lepetodrilidae	6.82
Hydroidolina	4.55
Cataegidae	4.22
Hesionidae	3.25
Top ten total	77.27

annelids at inner transition sites (Table 2), contributing 14.3% of the 68.4% dissimilarity (SIMPER) between active and inner transition sites; hesionid and lacydoniid polychaetes were the most abundant annelids at active sites (Table 2), contributing 6.7% of the dissimilarity. Gastropods mainly present at active sites also had a significant contribution to the dissimilarity between active and inner transition sites (Provannidae, Cataegidae, Neolepetopsidae). At outer transition sites, the community loses amphinomid, serpulid, lacydoniid, ampharetid, polynoid, and terebellid polychaetes completely. Cnidarians and peracarids were better represented at outer (16.3% and 23.2%, respectively) than inner transition (2.0% and 4.4%, respectively) sites. Among these, the groups that contributed the most to dissimilarity between inner and outer transition sites were hydroids and amphipods (SIMPER, average dissimilarity = 63.79%), which were more abundant at outer transition sites.

Table 2. Top ten taxa given as percent of the total for each seepage activity, based on densities for *in situ* carbonate rocks collected in different seepage regimes at Mound 12 in 2018.

Taxa	Percentage
2018 Active	
Cataegidae	11.97
Lacydoniidae	8.45
Hesionidae	7.75
Tanaiacea	7.04
Provannidae	4.93
Amphinomidae	4.23
Dorvilleidae	4.23
Chrysopetalidae	4.23
Ophiuroidea	4.23
Neolepetopsidae	4.23
Top ten total	61.27
2018 Inner transition	
Chrysopetalidae	56.51
Syllidae	6.62
Trombidiformes	5.08
Maldanidae	3.97
Amphipoda	2.87
Amphinomidae	2.21
Hesionidae	1.77
Hydroidolina	1.77
Lacydoniidae	1.55
Serpulidae	1.10
Top ten total	83.44
2018 Outer transition	
Chrysopetalidae	23.64
Hydroidolina	21.82
Amphipoda	16.36
Hesionidae	7.27
Maldanidae	5.45
Phyllococidae	3.64
Syllidae	3.64
Ostracoda	3.64
Dorvilleidae	1.82
Flabelligeridae	1.82
Top ten total	89.09

There was significant interannual variability in community composition (two-way ANOSIM, Global $R = 0.339$, $P = 0.001$; Fig. 2D). Several groups contributed to dissimilarity between years (sites combined) with greater abundance in 2017 including Lepetodrilidae, Neolepetopsidae, Cataegidae, Ophiuroidea, Anomura, Serpulidae, Hesionidae, Pyropeltidae, Tanaiacea, and Amphinomidae (SIMPER, average dissimilarity = 67.32; Tables 1, 2).

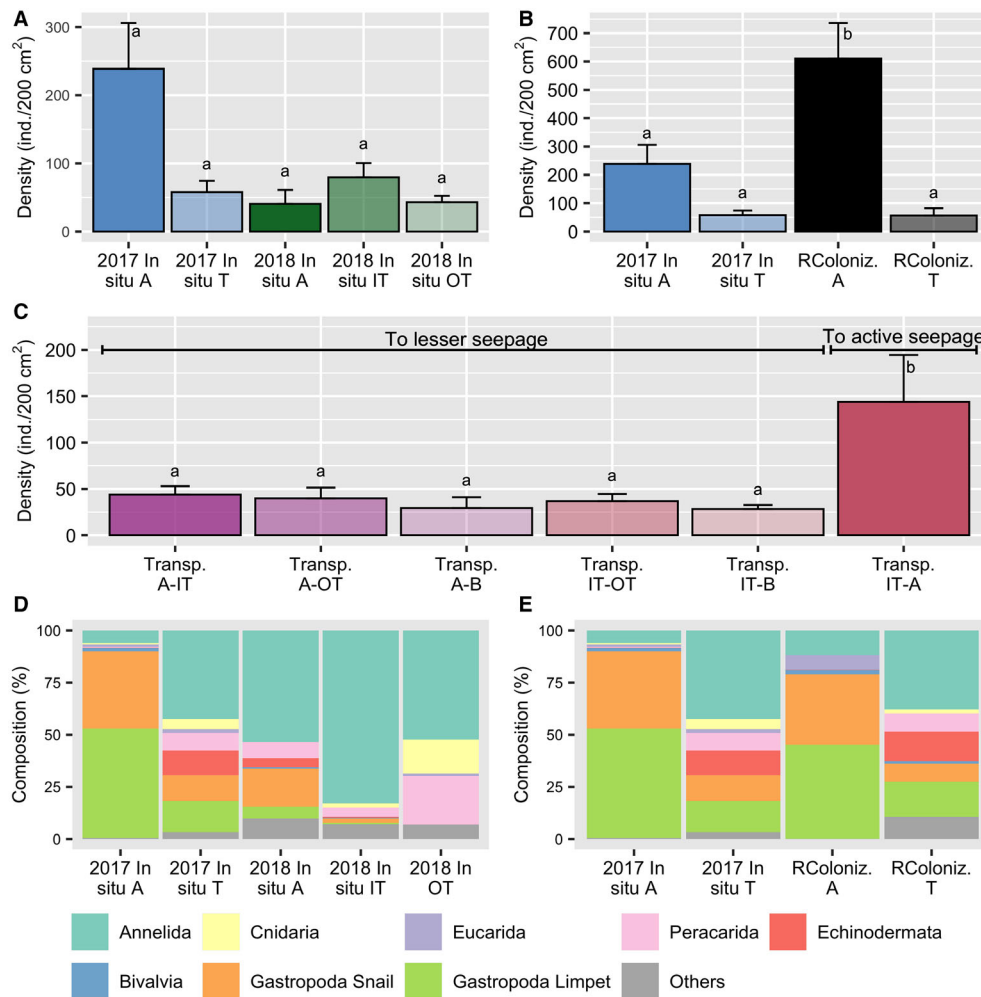


Fig. 2. Average \pm one standard error density of macrofaunal communities on (A) *in situ* carbonate rocks collected in different seepage regimes at Mound 12 in 2017 and 2018, and (B) carbonate rocks deployed at active and transition sites for 7.4 yr (2010–2017) (Rock colonization experiment—RColoniz.), and (C) carbonate rocks transplanted across seepage gradients for 17 months (2017–2018; Transplant experiment) from A-IT, A-OT, A-B, IT-OT, IT-B, IT-A. And community composition of macrofaunal major taxa on the same (D) *in situ* rocks, and (E) deployed rocks (Rock colonization experiment—RColoniz.). A: Active, T: Transition, IT: Inner transition, OT: Outer transition, B: Background.

Trophic structure.—In 2017 (Fig. 3A), mean $\delta^{13}\text{C}$ and $\delta^{15}\text{N}$ values were significantly lower ($\delta^{13}\text{C}$: $W = 825$, $P = 0.005$, $\delta^{15}\text{N}$: $W = 454.4$, $P < 0.001$) for macrofauna at active ($\delta^{13}\text{C} = -36.3 \pm 1.6\text{‰}$, $\delta^{15}\text{N} = 3.5 \pm 1.0\text{‰}$) than at transition sites ($\delta^{13}\text{C} = -27.9 \pm 2.9\text{‰}$, $\delta^{15}\text{N} = 9.2 \pm 1.1\text{‰}$; Table 3). Annelids had lower $\delta^{15}\text{N}$ values at active sites ($4.6 \pm 0.8\text{‰}$) than at transition sites ($9.6 \pm 0.9\text{‰}$; $W = 122$, $P < 0.001$), while limpets had lower $\delta^{13}\text{C}$ values at active ($-43.2 \pm 2.5\text{‰}$) than at

transition sites ($-29.9 \pm 1.7\text{‰}$; $W = 52$, $P = 0.02$; Appendix S1: Table S2).

In 2018 (Fig. 3B), similar patterns were observed; macrofauna at active sites had lower mean $\delta^{13}\text{C}$ ($-36.2 \pm 1.3\text{‰}$) and $\delta^{15}\text{N}$ ($6.2 \pm 0.8\text{‰}$) values than at inner transition ($\delta^{13}\text{C} = -33.7 \pm 2.7\text{‰}$, $\delta^{15}\text{N} = 7.9 \pm 0.6\text{‰}$; $\delta^{13}\text{C}$: $z = -2.52$, $P = 0.005$, $\delta^{15}\text{N}$: $z = -2.41$, $P = 0.01$), and outer transition sites ($\delta^{13}\text{C} = -25.6 \pm 0.1\text{‰}$, $\delta^{15}\text{N} = 9.4 \pm 0.3\text{‰}$; $\delta^{13}\text{C}$: $z = -4.05$, $P < 0.001$,

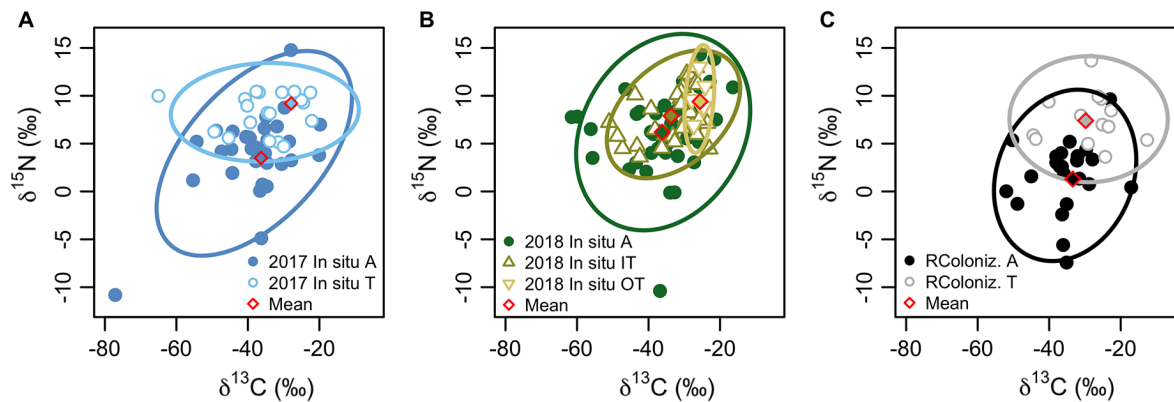


Fig. 3. Dual isotope plots reflecting macrofaunal invertebrate community trophic niche diversity based on corrected standard ellipse area on *in situ* carbonate rocks collected at active and transition sites at Mound 12 in (A) 2017 and (B) 2018, and (C) carbonate rocks deployed for 7.4 yr (2010–2017) at active and transition sites at Mound 12 (Rock colonization experiment—RColoniz.). Each point represents the average for one species.

$\delta^{15}\text{N}$: $z = -3.01$, $P = 0.004$). The $\delta^{13}\text{C}$ value was also lower at inner transition than at outer transition sites ($z = -2.64$, $P = 0.006$); the mean $\delta^{15}\text{N}$ was nearly significantly different ($z = -1.68$, $P = 0.05$; Table 3). However, mean $\delta^{13}\text{C}$ and $\delta^{15}\text{N}$ values were not significantly different at active vs transition sites for any individual taxon ($P > 0.05$, Appendix S1: Table S2).

At active sites, the mean $\delta^{13}\text{C}$ value of macrofauna was not significantly different between years ($W = 2019.5$, $P = 0.27$), but $\delta^{15}\text{N}$ was higher in 2018 than in 2017 ($W = 1433.5$, $P < 0.001$; Table 3). At transition sites, mean $\delta^{15}\text{N}$ was not significantly different between years ($\chi^2_2 = 3.45$, $P = 0.18$), but mean $\delta^{13}\text{C}$ was slightly higher at outer transition sites in 2018 than transition sites in 2017 ($z = -2.55$, $P = 0.008$; Table 3). Mean $\delta^{13}\text{C}$ values were not significantly different between years at active sites for limpets, snails, and annelids, but $\delta^{15}\text{N}$ values were higher for annelids in 2018 than 2017 ($W = 248$, $P = 0.01$; Appendix S1: Table S2). At transition sites, mean $\delta^{13}\text{C}$ and $\delta^{15}\text{N}$ values were not significantly different between years for any taxon ($P > 0.05$; Appendix S1: Table S2).

Active sites showed greater trophic diversity (higher range of $\delta^{13}\text{C}$ and $\delta^{15}\text{N}$, greater TA and SEAc) than transition sites in both years (Fig. 3A, B, Appendix S1: Table S3). Within active sites, trophic diversity was greater in 2017 than in 2018 (Appendix S1: Table S3).

Transplants across seepage gradient

Densities (Fig. 2C).—Densities of invertebrate macrofauna on rocks transplanted from active sites to inner transition sites (A-IT), to outer transition sites (A-OT), or to background sites (A-B) were significantly lower than the average density of communities on *in situ* rocks at active sites collected in 2017 at the start of the experiment (A-IT: $z = 2.26$, $P = 0.01$; A-OT: $z = 2.00$, $P = 0.02$; A-B: $W = 24$, $P = 0.01$), but densities were not different from those on the 2018 *in situ* rocks at their recovery sites. For the remaining transplant treatments from inner transition to active (IT-A), to outer transition (IT-OT) or to background sites (IT-B), densities on the transplanted rocks were not significantly different than on *in situ* rocks collected in 2017 at the initial site or *in situ* rocks collected in 2018 at the end site of the transplants (IT-A: $\chi^2_2 = 3.218$, $P = 0.20$; IT-OT: $\chi^2_2 = 1.618$, $P = 0.44$; IT-B: $W = 15$, $P = 0.28$). However, the average density on transplanted rocks tended to increase when the rocks were moved to more active sites (IT-A) and decrease when moved to sites with lesser seepage (IT-OT and IT-B). The transplant IT-A showed the highest faunal densities of all transplant treatments ($\chi^2_5 = 12.157$, $P = 0.03$).

Community composition (Fig. 4, Tables 4, 5).—Community composition on all the transplanted rocks was significantly different than on *in situ* rocks at their initial site in 2017 (ANOSIM,

Table 3. Mean \pm 1 standard error carbon and nitrogen stable isotope values (‰) of macrofauna on *in situ* carbonate rocks collected in different seepage regimes at Mound 12 in 2017 (AT37-13) and 2018 (AT42-03), carbonate rocks transplanted across seepage activity for 17 months (2017–2018), and carbonate rocks deployed at active and transition sites for 7.4 yr (2010–2017).

Seepage activity	No. species	$\delta^{13}\text{C}$ (‰)	$\delta^{15}\text{N}$ (‰)
In situ carbonate rocks			
2017 Active	32	-36.3 ± 1.6	3.5 ± 1.0
2017 Transition	22	-27.9 ± 2.9	9.2 ± 1.1
2018 Active	43	-36.2 ± 1.3	6.2 ± 0.8
2018 Inner Transition	32	-33.7 ± 2.7	7.9 ± 0.6
2018 Outer Transition	7	-25.6 ± 0.1	9.4 ± 0.3
Transplant experiment with carbonate rocks (17 months, 2017 to 2018)			
Inner Transition to Active (IT-A)	25	-39.1 ± 3.9	5.9 ± 1.3
Active to Inner Transition (A-IT)	26	-37.0 ± 4.6	6.8 ± 1.6
Active to Outer Transition (A-OT)	11	-37.7 ± 4.3	8.3 ± 1.0
Inner Transition to Outer Transition (IT-OT)	11	-29.4 ± 5.1	9.3 ± 0.8
Active to Background (A-B)	13	-45.3 ± 9.2	6.2 ± 1.2
Inner Transition to Background (IT-B)	9	-24.2 ± 1.4	9.9 ± 1.4
Rock Colonization experiment with defaunated carbonate rocks (7.4 yr, 2010 to 2017)			
Active	23	-33.4 ± 2.7	1.3 ± 1.0
Transition	13	-29.8 ± 1.8	7.4 ± 0.6

Note: Number of species represent specimens collected on board for isotope analyses and do not necessarily reflect total number of species present on the rocks.

$P < 0.05$ for all treatments), except for IT-A, but similar to the community on *in situ* rocks at their end site in 2018 (ANOSIM, $P > 0.05$ for all treatments). The community on the IT-A transplanted rocks (Fig. 4C) did not differ from the *in situ* transition community in 2017 nor from the *in situ* active community in 2018 (ANOSIM, Global $R = 0.123$, $P = 0.09$).

Rocks moved to transition sites (A-IT, A-OT, and IT-OT) each acquired 3 of the taxa unique to 2018 *in situ* inner/outer transition rocks (Fig. 5A, B, D); in 2018, there were 12 and 6 taxa unique to *in situ* inner and outer transition rocks, respectively (Fig. 5B, D). The transition fauna acquired on A-IT, A-OT, and IT-OT rocks consisted mainly of specialists such as capitellid, flabelligerid and lumbrinerid polychaetes, ostracods, and hydroids (Tables 4, 5, Appendix S1: Table S4). The transition specialists represent only 2–6% of individuals on these transplanted rocks, and most of the fauna found in 2018 on the rocks transplanted to transition sites were generalist taxa present at both active and transition sites.

Transition taxa appear to be tolerant to changing seepage. Nearly half (45%) of the 11 transition taxa (4% of individuals) on 2017 *in situ* transition rocks persisted on the IT-A transplanted rocks (Fig. 5C), and 42% of 21 taxa (16%

of individuals) persisted on the IT-OT transplanted rocks (Fig. 5D). Chrysopetalids, peracarids, and hydroids persisted through the transplant from IT-A, but serpulid polychaetes, mainly *Laminatubus* sp., did not (Table 5). When moved to background sites, 59% of the 34 taxa on 2017 *in situ* transition rocks persisted on the IT-B transplanted rocks in 2018 (Fig. 5F), with most of the individuals comprised of hydroids (Table 5, Appendix S1: Table S4).

In contrast, only 25% of the 12 active taxa unique to 2017 *in situ* active rocks (8% of individuals) persisted on the A-IT transplanted rocks (Fig. 5A), consisting of anomurans and mytilid, and nuculanid bivalves (Table 4, Appendix S1: Table S4). Paradoxically, the active fauna remained longer when transplanted to outer transition sites; 62% of the 29 active-only taxa that were present on 2017 *in situ* active rocks (43% of individuals) were also present on the A-OT transplanted rocks (Fig. 5B). The persistent active fauna included neolepetopsid limpets and ampharetid polychaetes that persisted in high densities, while provannid snails seemed not to survive the transplant from active sites to lesser seepage. Other active seep species were also found still alive 17 months after transplant to the transition area, such as *Laminatubus* sp.

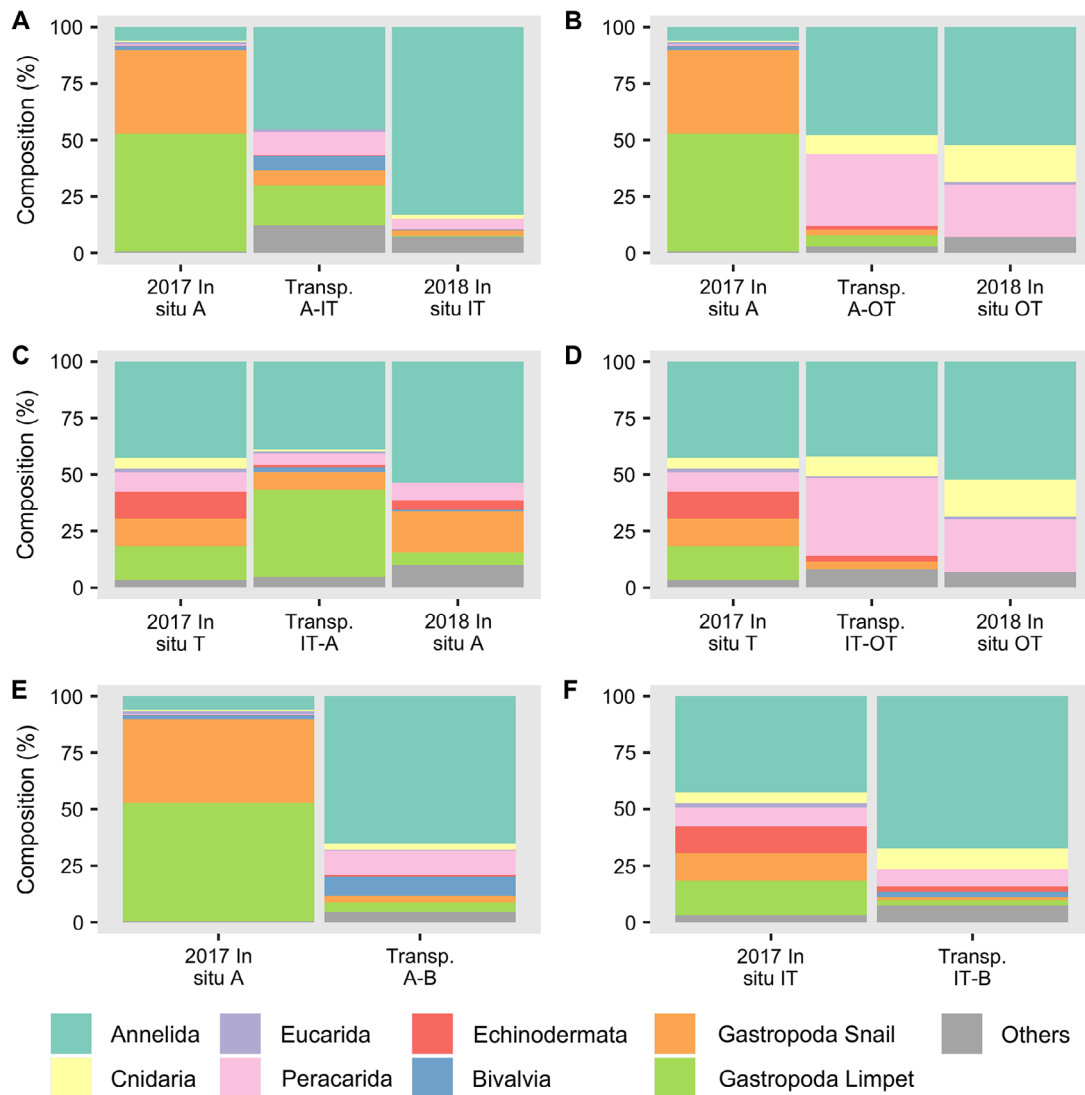


Fig. 4. Composition (%) of the macrofaunal invertebrate community on experimental carbonate rocks transplanted across seepage gradients for 17 months (2017–2018; Transplant experiment—Transp.) shown with *in situ* carbonate rocks at the initial site collected in 2017 and at the final site collected in 2018: (A) 2017 *in situ* active; transplant active to inner transition; 2018 *in situ* inner transition, (B) 2017 *in situ* active; transplant active to outer transition; 2019 *in situ* outer transition, (C) 2017 *in situ* transition; transplant inner transition to active; 2018 *in situ* active, (D) 2017 transition *in situ* transition; transplant inner transition to outer transition; 2018 *in situ* outer transition, (E) 2017 *in situ* active, transplant active to background, and (F) 2017 *in situ* transition; transplant inner transition to background. A: Active, T: Transition, IT: Inner transition, OT: Outer transition, B: Background. There were no *in situ* rocks at background sites.

(Serpulidae), *Archinome levinae* (Amphinomidae), and *Bathymodiolus* sp. (Mytilidae). When moved to background sites, 62% of the 42 taxa on 2017 *in situ* active rocks (22% of individuals) persisted on the A-B transplanted rocks (Fig. 5E),

including mainly cirratulidae and nereidid polychaetes and mytilid and nuculanidae bivalves (Table 4).

Active taxa were acquired on rocks transplanted from IT-A at a higher rate (70% of the

Table 4. Top ten taxa given as percent of the total for each treatment, based on densities on experimental carbonate rocks transplanted from active sites to inner transition (A-IT), outer transition (A-OT), and background (A-B) sites for 17 months (2017–2018) at Mound 12.

Taxa	Percentage
A-IT	
Chrysopetalidae	20.34
Neolepetopsidae	16.90
Mytilidae†	6.55
Trombidiformes	5.17
Tanaidacea	4.83
Cataegidae	4.83
Ampharetidae	4.48
Phyllodocidae	3.79
Amphipoda	3.45
Polyplacophora	3.45
Top ten total	73.79
A-OT	
Amphipoda	23.85
Chrysopetalidae	11.72
Amphinomidae†	9.21
Actinaria	8.37
Polynoidae†	6.28
Neolepetopsidae†	3.77
Nereididae†	3.35
Hydroidolina	3.35
Polyplacophora	2.93
Hesionidae‡	2.09
Top ten total	74.92
A-B	
Phyllodocidae	14.95
Ampharetidae	12.96
Amphipoda	9.30
Hesionidae	6.31
Amphinomidae	5.65
Cirratulidae†	5.32
Mytilidae†	4.65
Nereididae†	4.32
Nuculanidae†	3.99
Siboglinidae	2.99
Top ten total	70.44

† Taxa unique to the start site that persisted on the transplant.

‡ Taxa unique to the end site that was acquired with the transplant.

active taxa on 2018 *in situ* active rocks were present; Fig. 5C) than the acquisition of transition taxa described above. Species that colonized the IT-A transplanted rocks were mainly adults and juveniles of *Archinome levinae* (Amphinomidae), *Provanna laevis* (Provannidae),

Table 5. Top ten taxa given as percent of the total for each treatment, based on densities on experimental carbonate rocks transplanted from inner transition sites to active (IT-A), outer transition (IT-OT), and background (IT-B) sites for 17 months (2017–2018) at Mound 12.

Taxa	Percentage
IT-A	
Neolepetopsidae	36.12
Chrysopetalidae	21.43
Provannidae‡	4.58
Lacydoniidae	3.77
Tanaidacea	3.64
Hesionidae	3.37
Cataegidae	2.70
Trombidiformes	2.56
Syllidae	2.43
Lepetodrilidae†	2.29
Top ten total	82.89
IT-OT	
Isopoda	25.68
Chrysopetalidae	19.59
Amphipoda	6.08
Hydroidolina	5.41
Amphinomidae†	3.38
Actinaria	3.38
Polynoidae†	2.70
Paraonidae	2.70
Tanaidacea†	2.70
Ophiuroidea†	2.70
Top ten total	74.32
IT-B	
Chrysopetalidae	32.10
Amphinomidae	8.64
Phyllodocidae	8.64
Hydroidolina†	6.79
Cirratulidae	3.70
Tanaidacea	3.70
Aplacophora	3.70
Polynoidae	2.47
Ophiuroidea	2.47
Nuculanidae	2.47
Top ten total	74.68

† Taxa unique to the start site that persisted on the transplant.

‡ Taxa unique to the end site that was acquired with the transplant.

Paralepetopsis sp. (Neolepetopsidae), and *Neolepetopsis* sp. (Neolepetopsidae). Thus, many of the individuals colonizing or persisting on the transplanted rocks belonged to more generalist taxa that live at both active and transition sites (Tables 4, 5, Appendix S1: Table S4).

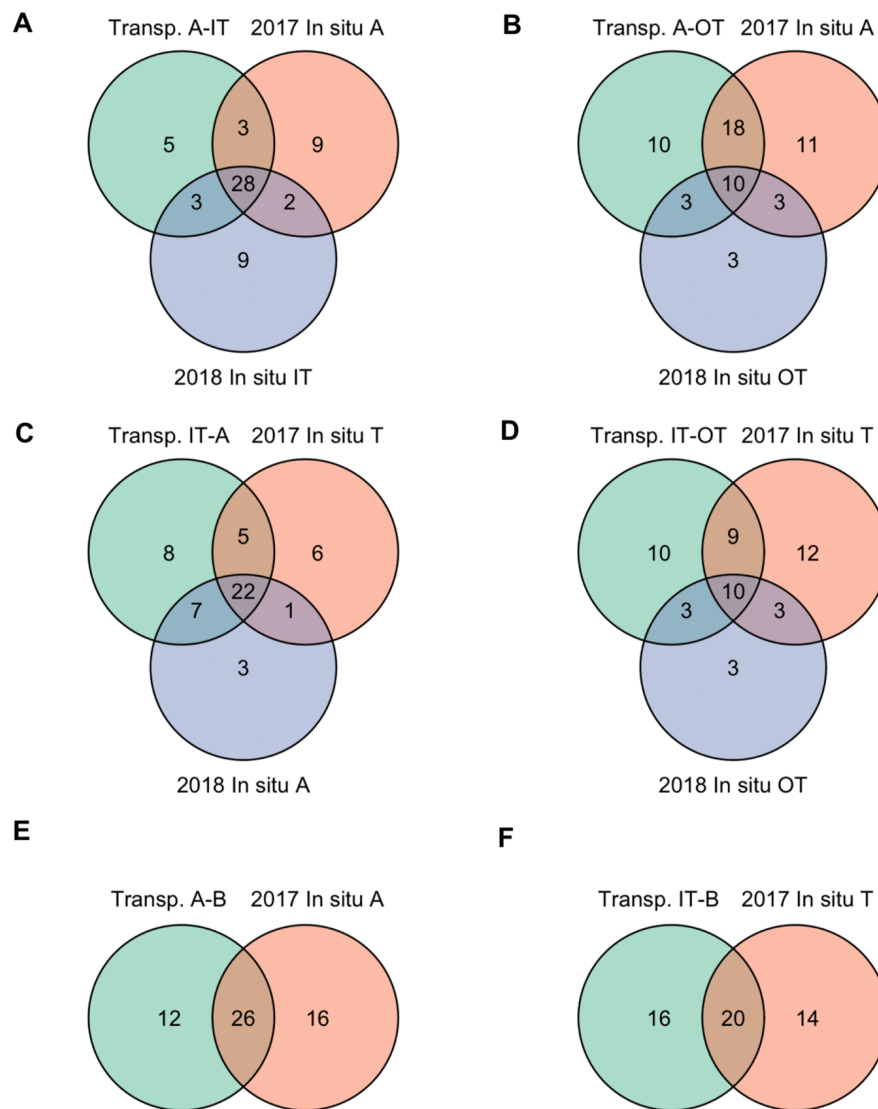


Fig. 5. Venn diagrams showing numbers of overlapping invertebrate taxa among macrofaunal communities on *in situ* carbonate rocks collected at active and transition sites at Mound 12 in 2017 and 2018, and on experimental carbonate rocks transplanted for 17 months (2017–2018) across seepage gradient (Transplant experiment—Transp.). Carbonates are shown for (A) 2017 *in situ* active; transplant active to inner transition; 2018 *in situ* inner transition, (B) 2017 *in situ* active; transplant active to outer transition; 2018 *in situ* outer transition, (C) 2017 *in situ* transition; transplant inner transition to active; 2018 *in situ* active, (D) 2017 transition *in situ* transition; transplant inner transition to outer transition; 2018 *in situ* outer transition, (E) 2017 *in situ* active, transplant active to background, and (F) 2017 *in situ* transition; transplant inner transition to background. A: Active, T: Transition, IT: Inner transition, OT: Outer transition, B: Background. There were no *in situ* background rocks available for study.

Trophic structure (Table 3).—Stable isotope values of macrofauna responded to changes in seepage over 17 months, though $\delta^{13}\text{C}$ was less sensitive to changes in seepage activity than

$\delta^{15}\text{N}$. Unexpectedly, the mean $\delta^{13}\text{C}$ value of animals on transplanted rocks was not significantly different than on *in situ* rocks at the start of the experiment in 2017 nor at the end in 2018, except

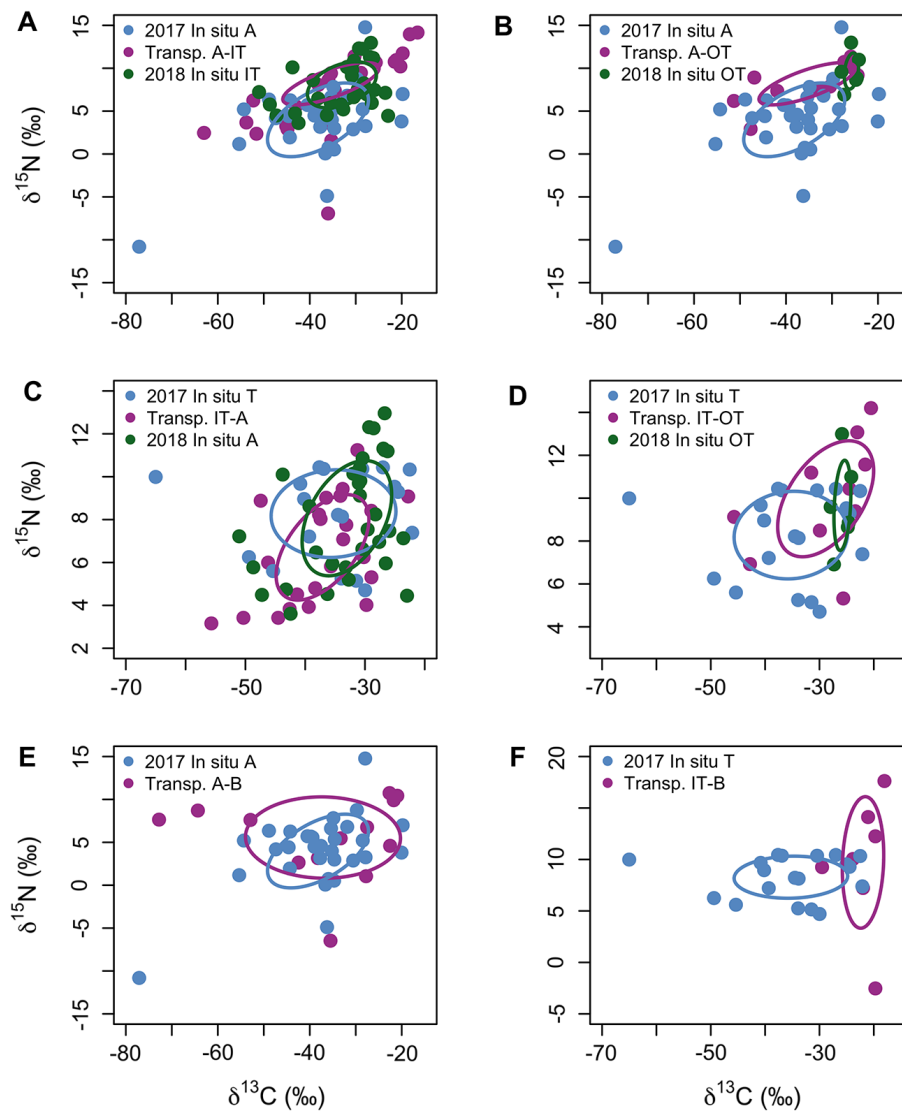


Fig. 6. Dual isotope plots reflecting macrofaunal invertebrate community trophic niche diversity on experimental authigenic carbonate rocks transplanted across seepage gradients for 17 months (2017–2018, Transplant experiment—Transp.; purple) shown with *in situ* carbonate rocks at the initial site collected in 2017 (blue) and at the final site collected in 2018 (green). (A) 2017 *in situ* active; transplant active to inner transition; 2018 *in situ* inner transition, (B) 2017 *in situ* active; transplant active to outer transition; 2019 *in situ* outer transition, (C) 2017 *in situ* transition; transplant inner transition to active; 2018 *in situ* active, (D) 2017 transition *in situ* transition; transplant inner transition to outer transition; 2018 *in situ* outer transition, (E) 2017 *in situ* active, transplant active to background, and (F) 2017 *in situ* transition; transplant inner transition to background. A: Active, T: Transition, IT: Inner transition, OT: Outer transition, B: Background. There were no *in situ* rocks at background sites. Each point represents the average for one species.

on rocks transplanted from A-OT where $\delta^{13}\text{C}$ was 12.1‰ lower than at the end site ($W = 12.5$, $P = 0.03$) and on rocks transplanted from IT-B

where $\delta^{13}\text{C}$ was 3.7‰ higher than the initial site ($W = 25$, $P < 0.001$; Table 3). Macrofaunal mean $\delta^{15}\text{N}$ value increased by 3.3‰ and 4.8‰ when

Table 6. Top ten taxa given as percent of the total for each seepage activity, based on colonizer densities for experimental carbonate rocks deployed at active and transition sites at Mound 12 for 7.4 yr (2010–2017).

Taxa	Percentage
Active	
Lepetodrilidae	33.61
Provannidae	27.58
Ampharetidae	8.01
Neolepetopsidae	7.89
Anomura	6.79
Hyalogyniridae	5.99
Pyropeltidae	3.54
Mytilidae	1.69
Phyllodocidae	1.31
Hesionidae	0.84
Top ten total	97.26
Transition	
Ophiuroidea	14.29
Neolepetopsidae	11.80
Serpulidae	9.94
Amphipoda	6.21
Aplacophora	4.97
Phyllodocidae	4.35
Cataegidae	4.35
Lepetodrilidae	4.35
Hesionidae	3.73
Lacydoniidae	3.11
Top ten total	67.08

rocks were transplanted from A-IT ($W = 266$, $P = 0.01$) and A-OT ($W = 266$, $P < 0.001$), respectively, and decreased by 2‰ when transplanted to active sites ($W = 136.5$, $P = 0.02$).

Macrofaunal $\delta^{13}\text{C}$ and $\delta^{15}\text{N}$ ranges, TA and SEAc (trophic diversity) were generally greater on rocks transplanted to lower seepage activity in comparison to *in situ* rocks at the end site of the experiment (Fig. 6). The opposite trend was observed for rocks transplanted from IT-A (Fig. 6 C, Appendix S1: Table S3).

For the majority of the different major taxa analyzed individually, isotopic composition was not significantly different among transplant treatments (Appendix S1: Table S2). An exception was in the limpets on rocks transplanted from A-OT sites; these had $\delta^{15}\text{N}$ values that were 6.2‰ higher than limpets of mostly the same species on *in situ* rocks collected in 2017 at active sites ($W = 38$, $P = 0.009$).

Colonization patterns on carbonate rocks

Densities (Fig. 2B).—The density of invertebrate macrofauna on colonizing carbonate rocks deployed for 7.4 yr (2010–2017) at active sites (610.7 ± 125.4 ind./200 cm²) was more than twice as high as on *in situ* rocks in 2017 at active sites (238.7 ± 67.3 ind./200 cm²; $W = 0$, $P = 0.03$), while at transition sites, colonizer densities (56.5 ± 25.7 ind./200 cm²) were not significantly different from those on 2017 *in situ* transition rocks (57.9 ± 16.5 ind./200 cm²; $W = 8$, $P = 1.00$). Colonizer density was more than 10× higher in 2017 (after 7 yr deployment) at active than transition sites ($W = 12$, $P = 0.05$); in contrast to the 2017 *in situ* rock densities that were 4× higher at active than transition sites. In terms of species presence, active colonizer fauna recovered more quickly than transition fauna, sharing 83% and 61% of taxa with *in situ* rocks at active and transition sites, respectively (Fig. 5).

Community composition (Fig. 2E).—The composition of the carbonate colonization communities was not significantly different than that of the communities on *in situ* rocks with similar seepage activity (ANOSIM, Global $R = -0.012$, $P = 0.48$), although the similarity between the 7.4-yr colonization community and the *in situ* community was greater at active (SIMPER, average similarity = 46.43) than at transition sites (SIMPER, average similarity = 35.08).

As with *in situ* rocks, community composition of colonizers changed with seepage activity (ANOSIM, Global $R = 0.464$, $P = 0.004$). Active sites were dominated by gastropods (45.0% limpets and 33.7% snails), and transition sites were dominated by annelids (37.9%), followed by limpets (16.8%) and echinoderms (14.3%). The gastropods Provannidae, Neolepetopsidae, Lepetodrilidae, and Pyropeltidae (more common at active sites where they composed 72.6% of the colonizer community; Table 6) were the main groups contributing to the dissimilarity between colonizers at active and transition sites (SIMPER, average dissimilarity = 72.38).

Trophic structure (Table 3).—On average, animals on colonization rocks exhibited the same isotopic patterns relative to seepage as those on *in situ* rocks, with lower mean $\delta^{13}\text{C}$ and $\delta^{15}\text{N}$ values at active ($\delta^{13}\text{C} = -33.4 \pm 2.7\text{‰}$, $\delta^{15}\text{N} = 1.3 \pm 1.0\text{‰}$) than at transition sites ($\delta^{13}\text{C} = -29.8 \pm 1.8\text{‰}$, $\delta^{15}\text{N} = 7.4 \pm 0.6\text{‰}$; $\delta^{13}\text{C}$: $W = 244$,

$P = 0.02$, $\delta^{15}\text{N}$: $W = 79$, $P < 0.001$). At active sites, mean $\delta^{13}\text{C}$ value was not significantly different between the community on colonization and *in situ* rocks ($W = 1299$, $P = 0.18$), but mean $\delta^{15}\text{N}$ was significantly higher on *in situ* rocks than on colonization rocks ($W = 2139.5$, $P < 0.001$). At transition sites, mean $\delta^{13}\text{C}$ and $\delta^{15}\text{N}$ values were not significantly different for the colonizing community than on *in situ* rocks ($\delta^{13}\text{C}$: $W = 268$, $P = 0.38$, $\delta^{15}\text{N}$: $W = 343$, $P = 0.61$). Annelids were the only taxon that showed different isotopic composition between active and transition sites and between colonization and *in situ* rocks, with lower mean $\delta^{15}\text{N}$ values at active than transition sites on colonization rocks ($W = 0$, $P < 0.001$), and lower mean $\delta^{15}\text{N}$ values at active sites on colonization rocks than on *in situ* rocks ($W = 94$, $P = 0.01$; Appendix S1: Table S2).

The community on colonization rocks exhibited greater trophic diversity at active than at transition sites, but at active sites the colonizer trophic diversity was lower than on *in situ* rocks in 2017 (Fig. 4C, Appendix S1: Table S3). The opposite trend was observed at transition sites, where the community on colonization rocks showed larger trophic diversity (TA and SEAc) than on *in situ* rocks in 2017 (Appendix S1: Table S3).

DISCUSSION

Resistance and resilience under manipulated and natural declining seepage

Seepage exhibits a strong influence on carbonate community composition (Tables 1, 2, Fig. 2). This is reflected in community-wide trophic patterns based on $\delta^{13}\text{C}$ and $\delta^{15}\text{N}$ (Table 3, Fig. 3, Appendix S1: Table S3), but not in taxon-specific isotopic signatures, which are stable across seepage gradients (Appendix S1: Table S2). These results are generally consistent with previous work on Pacific seep carbonates (e.g., Levin et al. 2015, 2017) and sediment faunas of Mound 12 (Ashford et al. 2021). Some methane use by invertebrates persists when obvious signs of seepage are absent, as indicated by low $\delta^{13}\text{C}$ at transition sites, consistent with studies showing that microbial activity continues in carbonate rocks after cessation of seepage (Marlow et al. 2014a, Case et al. 2015).

The community on carbonate rocks that was transplanted from active sites to lesser seepage

activity did not retain the characteristics (community composition—i.e., identities of the taxa present in the community— density and trophic structure) of “active communities” (Fig. 1C, 4, 5, 6). However, survivors retained their low $\delta^{13}\text{C}$ values from chemosynthetic sources and acquired higher $\delta^{15}\text{N}$ values from photosynthetic sources, possibly reflecting a faster turnover of $\delta^{15}\text{N}$ than $\delta^{13}\text{C}$ in animal tissues. Previous studies have found differences in turnover rates of $\delta^{15}\text{N}$ and $\delta^{13}\text{C}$, although they have not been consistent, and isotope tissue shifts may vary as a function of food quality, taxon, and tissue type (see Mayor et al. 2010, Thurber 2014, deVries et al. 2015, Vander Zanden et al. 2015, Lecea et al. 2016). Similar responses were observed in a 13-mo transplant experiment at Hydrate Ridge, Oregon, where the transplanted rocks took on the dominant species and abundance patterns of their new sites (Levin et al. 2017) and shifted isotope signatures (Grupe 2014).

Several taxa appear more attracted to rocks under conditions of reduced seepage. While the lower toxicity levels could explain their preference, diet preferences and habitat usage may as well. The high abundance of chrysopetalids, known to be carnivores, scavengers (Boggeman 2009) or bacterial grazers (Wiklund et al. 2009), on rocks transplanted from active sites to lesser seepage activity may reflect consumption of bacteria or meiofauna that persisted or died after being transplanted to lesser seepage (Levin et al. 2017). In contrast, peracarid crustaceans (amphipods, tanaids, and isopods), also found in high abundance on rocks transplanted to lesser seepage activity, were probably not consuming the chemosynthesis-derived production on the rocks based on their high isotope values, but were potentially obtaining substrate, habitat, and nursery sites, as many tube/burrow-dwelling peracarids provide extended parental care (Thiel 1999) and we found many juveniles and gravid females.

Native seep gastropods are commonly microbial grazers and thus likely to respond to changes in the microbial flora associated with the carbonates (Levin et al. 2017). Case et al. (2015) observed 30% lower microbial operational taxonomic unit (OTU) richness on rocks transplanted from active to inactive sites at Hydrate Ridge and some new OTUs were acquired. On rocks transplanted to lesser seepage, provannid snails

did not survive whereas neolepetopsid limpets exhibited high abundance and persistence in declining seepage, potentially facilitated by their diet flexibility. Limpets may feed on the remaining or newly acquired microbes within the rocks (Zapata-Hérmendez et al. 2014), retaining their low $\delta^{13}\text{C}$ values, as well as on POC or the newly settled invertebrates that colonized the rock at transition sites (Fretter 1990), yielding higher $\delta^{15}\text{N}$ values.

Among the other seep species that survived the transplant to lesser seepage (*Laminatubus* sp., *Archinome levinae*, and *Bathymodiolus* sp.), *Bathymodiolus* sp. is known to have endosymbiotic methanotrophic bacteria in its gills (Duperron et al. 2005), and *Laminatubus* sp. farms methanotrophic bacteria in its tentacular crown (Goffredi et al. 2020). Persistence of these bacteria, which are capable of fixing local nitrogen, could explain the extremely low $\delta^{15}\text{N}$ values of bivalves on transplanted rocks from active sites to lesser seepage. However, mytilid mussels can also filter-feed on phytoplankton-based detritus (Riekenberg et al. 2016), and the slow tissue turnover of C and N, reported for *B. childressi* as being longer than 1 yr (Dattagupta et al. 2004), could reduce the likelihood of a shift in isotopic composition in the transplanted mussels we studied.

Slow carbon tissue turnover resulting from a change in chemosynthetic production rates could also explain why the average $\delta^{13}\text{C}$ values for different taxa and for the total active community were not significantly different between 2017 and 2018 (except for annelids; Table 3). This is in contrast to the interannual shift in community composition on *in situ* rocks, with lower abundances of native seep species (lepetodrilid and neolepetosid limpets, yeti crab *Kiwa puravida*, and provannid snails) at active sites suggestive of a decline in seepage activity (Fig. 2). This pattern was also observed on the transplants to lesser seepage. In addition, the higher average $\delta^{15}\text{N}$ for macrofauna at active sites in 2018 as compared to 2017 (Table 3) suggests a lower contribution of chemosynthetic production to their diets.

Additional effects that lead us to infer there was a natural decline in seepage activity between 2017 and 2018 include declining total faunal density and gastropod density at active sites in 2018, with values more comparable to transition site densities observed at Mound 12 in 2009 (Grupe

et al. 2015, Levin et al. 2015) and 2017 (this study). The observed dynamics driven by interannual fluctuations in methane may be common in this setting, as natural variations of water column methane concentration within 12 months have been reported along the Costa Rican margin (Mau et al. 2007). Strong, repeated earthquake-related perturbations are common in the region (Xie et al. 2020); these could modulate methane seepage.

Resistance and resilience under a manipulated rise in seepage

When carbonate rocks were transplanted from transition to active sites, we observed a rapid (17 mo) colonization of grazers characteristic of active sites, such as *Provanna laevis* (Provannidae), *Paralepetopsis* sp. (Neolepetopsidae), and *Neolepetopsis* sp. (Neolepetopsidae) (Tables 4, 5). The slightly lower $\delta^{15}\text{N}$ values for these animals, as compared to those on *in situ* rocks at active sites (Table 3), suggest the rapid establishment and growth of a diverse microbial community that provides their food, consistent with observations by Case et al. (2015) and Levin et al. (2017) at Hydrate Ridge after 13-month transplant experiments. We predicted that active seepage could create an environment toxic to transplanted transition species. However, the presence of chrysopetalids, peracarids, and hydroids on rocks transplanted to active sites after 17 months suggests that, instead, they can persist under active seepage. The unexpected coexistence of these transition species and active species yielded the highest faunal densities of all transplants, a pattern also observed by Levin et al. (2017) at Hydrate Ridge. The serpulid *Laminatubus* sp. was an exception; despite high abundance at transition sites, it did not thrive on the rocks transplanted to active sites. Notably, other species of serpulids have been reported at high densities at or near active seepage in Costa Rica (Levin et al. 2012), Santa Monica Basin (Georgieva et al. 2019), and in the Greenland Sea (Vinn et al. 2013, 2014).

Colonization rates and trajectory on carbonate rocks

To test the longer-term colonization rates of seep and non-seep communities, defaunated rocks were deployed at active and transition sites for 7.4 yr (2010–2017). As on *in situ* rocks, the

density of colonists was higher at active than transition sites, and the observed density overshoot on 7.4-yr colonization rocks compared to *in situ* rocks (4× higher; Fig. 2) was also reported by Grupe (2014) on a 10.5-months colonization experiment at Mound 12. Recruitment may be enhanced by the absence of predators on colonization rocks, but it is surprising to see this effect persist after 7.4 yr.

The most abundant colonizers at active sites (provannid, lepetodrilid, neolepetopsid, and pyropeltid gastropods along with yeti crabs) were also among the most abundant groups on *in situ* rocks, suggesting community recovery by taxa that may be both good colonizers and competitors. The reduced macrofaunal dietary niche observed on the colonization rocks may derive from a diet of microbes that did not attain its normal diversity and structure in 7.4 yr. Some evidence for a dietary shift among colonizers was seen in limpets, and similar shifts were observed in the transplant experiments. This dietary flexibility appears to be lacking in grazing Provannidae. They were absent on colonization rocks at transition sites (Levin and Sibuet 2012, Van Dover et al. 2012) but had high abundance on *in situ* rocks at transition sites, suggesting availability of larvae was not an impediment for their colonization. In contrast, the rapid colonization of bacterial grazers (including Provannidae) and their low $\delta^{15}\text{N}$ values on rocks transplanted to active sites are likely a result of the rapid establishment and growth of the microbial community that provides their food.

At bathyal seeps off both Costa Rica and Oregon, carbonate fauna appear to colonize or recover more quickly at active than transition sites based on short (10-, 13-, 17 months) and longer (7.4-yr) colonization and transplant experiments as shown here and in Grupe (2014), Levin et al. (2015), and Levin et al. (2017). Active seep fauna also remains longer and are more likely to retain their distinctive isotope signatures when transplanted to sites with reduced seepage than the fauna in the reciprocal transplant (Grupe 2014, Levin et al. 2017). The rapid colonization is probably due to the higher chemosynthetic production (i.e., microbial availability) associated with active seepage, as well as the habitat complexity created by the carbonates. However, the persistence of native seep fauna in the transition

zones, where they are typically uncommon, may be due to the continuation of chemosynthetic productivity within the transplanted carbonates (Marlow et al. 2014a). These observations highlight the importance of fluid seepage and its variability in shaping density and diversity through the provision of microbial food resources, geochemical toxicity, or hard substrate availability for settlement (Grupe 2014).

Dynamics and implications for conservation and management

Ecological succession at hydrothermal vents can occur over time scales of months to years, likely driven by rapid microbial recovery (Tunnicliffe et al. 1997, Shank et al. 1998, Marcus et al. 2009). The tubeworm *Ridgea pisceasae*, an ecosystem engineer at vents, achieves densities and lengths typical of mature vents within 1–3 yr post-eruption (Marcus et al. 2009) and at newly formed vents (Shank et al. 1998), supporting high species diversity of the associated invertebrate community. In contrast, succession at hydrocarbon seeps is thought to occur on annual, decadal, or century time scales (Cordes et al. 2009). However, these patterns are derived from studies utilizing a space-for-time substitution and not on experimental evidence, and therefore, it is difficult to draw conclusions about finer scale temporal changes.

In the present study at a seep site, 7.4 yr did not yield full recovery of the invertebrate community on bare carbonate rocks. However, 17 months was enough time for the community to take on the composition and structure of the local community on transplanted rocks hosting microbes and animals and key community elements persisted even when transplanted to lower seepage conditions. Thus, it is clear that colonizing fauna at chemosynthetic ecosystems respond to an initial development of habitat complexity and food availability on varied time scales, and recovery at seeps can be rapid as long as a source of recruits and/or dietary resources are available. Active fauna at Mound 12 recovered more quickly than transition fauna (this study), probably due to the higher chemosynthetic production and microbial biomass associated with active seepage, as well as the habitat complexity created by the carbonates.

The understanding of deep-sea ecosystem dynamics through studies of survival and

colonization rates using either experimental approaches (such as colonization and transplant experiments performed here) or natural geological phenomena (e.g., volcanic eruptions and earthquakes affecting seepage) offer valuable information on resilience, as deep-sea ecosystems are increasingly susceptible to natural and anthropogenic disturbances (Ramirez-Llodra et al. 2011, Levin and Sibuet 2012, Mengerink et al. 2014). More specifically, methane seeps are often associated with the presence of oil and gas extraction activities and occur on slopes where bottom fish are harvested commercially (Amon et al. 2017, Bernardino et al. 2020). Although some measures for conservation of seeps have been implemented in the past (see Cordes et al. 2016, NOAA 2020), given the ecological interactions between native seep and background communities (Cordes et al. 2005, Demopoulos et al. 2010, Levin et al. 2016, Ashford et al. 2021), we suggest seeps should be given formal protection measures. Risk assessments should incorporate the different vulnerabilities and sensitivities among taxa and trophic groups (Rowden et al. 2016). Transition zones should also be considered in spatial management, noting that they may function as a potential pool of colonizers for a disturbed seep and vice-versa.

CONCLUSION

Understanding the contributions of seep ecosystems to continental margin biodiversity, ecosystem dynamics, and community functioning advances fundamental science as well as our ability to manage these systems. Here, we observed short-term, between-year variability in invertebrate macrofaunal communities on carbonate rocks and their trophic structure due to natural changes in environmental context (i.e., seepage activity, habitat complexity, and food availability based on chemosynthetic production). Macrofauna experiencing experimentally induced changes in seepage activity and colonizing carbonate rocks illustrate short-term (17 months) and long-term (7.4 yr) responses that change along spatial gradients, where fauna closer to active seepage (native seep fauna) emerge and recover faster than transition fauna (characterized by the coexistence of seep and background faunas). In addition, macrofaunal

responses seem to be dictated by the availability of source recruits and dietary resources promoted by habitat complexity, especially in the long term. These observations highlight the interaction between the seep and the surrounding deep-sea community promoted by carbonate rocks, the contribution of seepage in determining deep-sea macrofaunal diversity, and the importance of habitat complexity and food availability in successional dynamics and vulnerability. These are crucial for predicting responses to disturbance arising from changing seepage activity or through anthropogenic activity. As human activities such as bottom fishing, or oil, gas, and mineral extraction increase on continental margins (Levin and Sibuet 2012, Van Dover et al. 2012, Bernardino et al. 2020), they will deeply impact habitat complexity, potentially affecting the macrofaunal community on longer timescales than at other chemosynthetic ecosystems. Such ecosystem interactions should be considered when planning for deep-sea biodiversity management and the designation of deep-water protected areas.

ACKNOWLEDGMENTS

This work was made possible through the efforts of many aboard RV Atlantis legs AT 37-13 and AT 42-03, including the captains, crew, pilots, and technicians of HOV Alvin, and science parties. Special thanks extended to O. Ashford, G. W. Rouse, V. Orphan, and S. Goffredi. This work was funded by National Science Foundation grant number OCE 1635219. OSP received a Scholarship award from the Association of Women in Science San Diego (2018). We would like to thank the Costa Rica Ministerio de Ambiente y Energía (Sistema Nacional de Áreas de Conservación/Comisión Nacional para la Gestión de la Biodiversidad) for granting collection permits (AT37-13: SINAC-CUS-PIR-035-2017, AT42-03: SINAC-SE-064-2018). OSP is forever grateful to her family for their support.

LITERATURE CITED

- Aloisi, G., C. Pierre, J.-M. Rouchy, J.-P. Foucher, and J. Woodside. 2000. Methane-related authigenic carbonates of eastern Mediterranean Sea mud volcanoes and their possible relation to gas hydrate destabilisation. *Earth and Planetary Science Letters* 184:321–338.
- Amon, D. J., J. Gobin, C. L. Van Dover, L. A. Levin, L. Marsh, and N. A. Raineault. 2017. Characterization

- of methane-seep communities in a deep-sea area designated for oil and natural gas exploitation off Trinidad and Tobago. *Frontiers in Marine Science* 4:342.
- Ashford, O. S., et al. 2021. A chemosynthetic ecotone – ‘chemotone’ – in the sediments surrounding deep-sea methane seeps. *Limnology and Oceanography* 66:1687–1702.
- Bahr, A., T. Pape, G. Bohrmann, A. Mazzini, M. Haeckel, A. Reitz, and M. Ivanov. 2009. Authigenic carbonate precipitates from the NE Black Sea: a mineralogical, geochemical, and lipid biomarker study. *International Journal of Earth Sciences (Geologische Rundschau)* 98:677–695.
- Benjamini, Y., and Y. Hochberg. 1995. Controlling the false discovery rate: a practical and powerful approach to multiple testing. *Journal of the Royal Statistical Society. Series B (Methodological)* 57:289–300.
- Bernardino, A. F., E. E. Cordes, and T. A. Schlacher. 2020. The natural capital of offshore oil, gas, and methane hydrates in the World Ocean. *in* M. Baker, E. Ramirez-Llodra, and P. Tyler, editors. *Natural capital and exploitation of the deep ocean*. Oxford University Press, Oxford, UK.
- Boetius, A., K. Ravenschlag, C. J. Schubert, D. Rickert, F. Widdel, A. Gleseke, R. Amann, B. B. Jørgensen, U. Witte, and O. Pfannkuche. 2000. A marine microbial consortium apparently mediating anaerobic oxidation of methane. *Nature* 407:623–626.
- Boetius, A., and F. Wenzhoefer. 2013. Seafloor oxygen consumption fuelled by methane from cold seeps. *Nature Geoscience* 6:725–734.
- Boggeman, M. 2009. Polychaetes (Annelida) of the abyssal SE Atlantic. *Organisms Diversity & Evolution* 9:251–428.
- Bowden, D. A., A. A. Rowden, A. R. Thurber, A. R. Baco, L. A. Levin, and C. R. Smith. 2013. Cold seep epifaunal communities on the Hikurangi Margin, New Zealand: composition, succession, and vulnerability to human activities. *PLOS ONE* 8:e76869.
- Case, D. H., A. L. Pasulka, J. J. Marlow, B. M. Grupe, L. A. Levin, and V. J. Orphan. 2015. Methane seep carbonates host distinct, diverse, and dynamic microbial assemblages. *MBio* 6:e01348–e1315.
- Clarke, K. R., and R. N. Gorley. 2015. *Primer7 v7: user manual/tutorial*. PRIMER-E Ltd, Plymouth.
- Cordes, E. E., et al. 2016. Environmental impacts of the deep-water oil and gas industry: a review to guide management strategies. *Frontiers in Environmental Science* 4:58.
- Cordes, E. E., D. C. Bergquist, and C. R. Fisher. 2009. Macro-ecology of Gulf of Mexico cold seeps. *Annual Review of Marine Science* 1:143–168.
- Cordes, E. E., S. Hourdez, B. L. Predmore, M. K. Redding, and C. R. Fisher. 2005. Succession of hydrocarbon seep communities associated with the long-lived foundation species *Lamellibrachia luy-mesi*. *Marine Ecology Progress Series* 305:17–29.
- Dattagupta, S., D. C. Bergquist, E. B. Szalai, S. A. Macko, and C. R. Fisher. 2004. Tissue carbon, nitrogen, and sulfur stable isotope turnover in transplanted *Bathymodiolus childressi* mussels: relation to growth and physiological condition. *Limnology and Oceanography* 49:1144–1151.
- Demopoulos, A. W. J., D. Gualtieri, and K. Kovacs. 2010. Food-web structure of seep sediment macrobenthos from the Gulf of Mexico. *Deep-Sea Research Part II* 57:1972–1981.
- deVries, M. S., C. M. del Rio, T. S. Tunstall, and T. E. Dawson. 2015. Isotopic incorporation rates and discrimination factors in mantis shrimp crustaceans. *PLOS ONE* 10:e0122334.
- Doya, C., D. Chatzievangelou, N. Bahamon, A. Purser, F. C. De Leo, S. K. Juniper, L. Thomsen, and J. Aguzzi. 2017. Seasonal monitoring of deep-sea megabenthos in Barkley Canyon cold seep by internet operated vehicle (IOV). *PLOS ONE* 12:e0176917.
- Dubilier, N., C. Bergin, and C. Lott. 2008. Symbiotic diversity in marine animals: the art of harnessing chemosynthesis. *Nature Reviews Microbiology* 6:725–740.
- Duperron, S., T. Nadalig, J.-C. Caprais, M. Sibuet, A. Fiala-Médioni, R. Amann, and N. Dubilier. 2005. Dual symbiosis in a *Bathymodiolus* sp. mussel from a methane seep on the Gabon continental margin (Southeast Atlantic): 16S rRNA phylogeny and distribution of the symbionts in gills. *Applied and Environmental Microbiology* 71:1694–1700.
- Fretter, V. 1990. The anatomy of some new archaeogastropod limpets (Order Patellogastropoda, Suborder Lepetopsina) from hydrothermal vents. *Journal of Zoology* 222:529–555.
- Fujikura, K., S. Kojima, K. Tamaki, Y. Maki, J. Hunt, and T. Okutani. 1999. The deepest chemosynthesis-based community yet discovered from the hadal zone, 7326 m deep, in the Japan Trench. *Marine Ecology Progress Series* 190:17–26.
- Georgieva, M. N., C. K. Paull, C. T. S. Little, M. McGann, D. Sahy, D. Condon, L. Lundsten, J. Pewsey, D. W. Caress, and R. C. Vrijenhoek. 2019. Discovery of an extensive deep-sea fossil a serpulid reef associated with a cold seep, Santa Monica Basin, California. *Frontiers in Marine Science* 6:115.
- Girard, F., J. Sarrazin, and K. Olu. 2020. Impacts of an eruption on cold-seep microbial and faunal dynamics at a mud volcano. *Frontiers in Marine Science* 7:241.
- Goffredi, S. K., et al. 2020. Methanotrophic bacterial symbionts fuel dense populations of deep-sea

- feather duster worms (Sabellida, Annelida) and extend the spatial influence of methane seepage. *Science Advances* 6:eay8562.
- Grupe, B. M. 2014. Implications of environmental heterogeneity for community structure, colonization, and trophic dynamics at Eastern Pacific Methane Seeps. Dissertation. University of California, San Diego, La Jolla, California, USA.
- Grupe, B. M., M. L. Krach, A. L. Pasulka, J. M. Maloney, L. A. Levin, and C. A. Frieder. 2015. Methane seep ecosystem functions and services from a recently discovered southern California seep. *Marine Ecology* 36:91–108.
- House, C. H., V. J. Orphan, K. A. Turk, B. Thomas, A. Pernthaler, J. M. Vrentas, and S. B. Joye. 2009. Extensive carbon isotopic heterogeneity among methane seep microbiota. *Environmental Microbiology* 11:2207–2215.
- Jackson, A. L., R. Inger, A. C. Parnell, and S. Bearhop. 2011. Comparing isotopic niche widths among and within communities: SIBER-Stable Isotope Bayesian Ellipses. *R. Journal of Animal Ecology* 80:595–602.
- Klaucke, I., D. G. Masson, C. J. Petersen, W. Weinrebe, and C. R. Ranero. 2008. Multifrequency geoaoustic imaging of fluid escape structures offshore Costa Rica: implications for the quantification of seep processes. *Geochemistry, Geophysics, Geosystems* 9:Q04010.
- Layman, C. A., D. A. Arrington, C. G. Montaña, and D. M. Post. 2007. Can stable isotope ratios provide for community-wide measures of trophic structure? *Ecology* 88:42–48.
- Lecea, A. M., A. J. Smit, and S. T. Fennessy. 2016. Riverine dominance of a nearshore marine demersal food web: evidence from stable isotope and C/N ratio analysis. *African Journal of Marine Science* 38(sup1):S181–S192.
- Levin, L. A., et al. 2012. A hydrothermal seep on Costa Rica margin: middle ground in a continuum of reducing ecosystems. *Proceedings of the Royal Society B-Biological Sciences* 279:2580–2588.
- Levin, L. A., et al. 2016. Hydrothermal vents and methane seeps: rethinking the sphere of influence. *Frontiers in Marine Science* 3:72.
- Levin, L. A., and G. F. Mendoza. 2007. Community structure and nutrition of deep methane seep macrofauna from the Aleutian Margin and Florida Escarpment, Gulf of Mexico. *Marine Ecology* 28:131–151.
- Levin, L. A., G. F. Mendoza, and B. M. Grupe. 2017. Methane seepage effects on biodiversity and biological traits of macrofauna inhabiting authigenic carbonates. *Deep-Sea Research Part II* 137: 26–41.
- Levin, L. A., G. F. Mendoza, B. M. Grupe, J. P. Gonzalez, B. Jellison, G. W. Rouse, A. R. Thurber, and A. Waren. 2015. Biodiversity on the rocks: Macrofauna inhabiting authigenic carbonate at Costa Rica methane seeps. *PLOS ONE* 10:e0131080.
- Levin, L. A., G. F. Mendoza, T. Konotchick, and R. Lee. 2009. Community structure and trophic relationships in Pacific hydrothermal sediments. *Deep Sea Research Part II* 56:1632–1648.
- Levin, L. A., and R. H. Michener. 2002. Isotopic evidence for chemosynthetic-based nutrition of macrobenthos: the lightness of being at Pacific methane seeps. *Limnology and Oceanography* 47:1336–1345.
- Levin, L. A., and M. Sibuet. 2012. Understanding continental margin biodiversity: a new imperative. *Annual Review in Marine Science* 4:79–112.
- Linke, P., K. Wallmann, E. Suess, C. Hensen, and G. Rehder. 2005. In situ benthic fluxes from an intermittently active mud volcano at the Costa Rica convergent margin. *Earth and Planetary Science Letters* 235:79–95.
- Marcus, J., V. Tunnicliffe, and D. A. Butterfield. 2009. Post-eruption succession of macrofaunal communities at diffuse flow hydrothermal vents on Axial Volcano, Juan de Fuca Ridge, Northeast Pacific. *Deep-Sea Research Part II* 56:1586–1598.
- Marlow, J. J., J. A. Steele, D. H. Case, S. A. Connon, L. A. Levin, and V. J. Orphan. 2014a. Microbial abundance and diversity patterns associated with sediments and carbonates from the methane seep environments of Hydrate Ridge. *OR. Frontiers in Marine Science* 1:44.
- Marlow, J. J., J. A. Steele, W. Ziebis, A. R. Thurber, L. A. Levin, and V. J. Orphan. 2014b. Carbonate-hosted methanotrophy represents an unrecognized methane sink in the deep sea. *Nature Communications* 5:5094.
- Mau, S. H., G. Rehder, I. G. Arroyo, J. Grossler, and E. Suess. 2007. Indications of a link between seismotectonics and CH₄ release from seeps off Costa Rica. *Geochemistry, Geophysics, Geosystems* 8: Q04003.
- Mau, S., H. Sahling, G. Rehder, E. Suess, P. Linke, and E. Soeding. 2006. Estimates of methane output from mud extrusions at the erosive convergent margin off Costa Rica. *Marine Geology* 225:129–144.
- Mayor, D. J., K. Cook, B. Thornton, P. Walsham, U. F. M. Witte, A. F. Zuur, and T. R. Anderson. 2010. Absorption efficiencies and basal turnover of C, N and fatty acids in a marine Calanoid copepod. *Functional Ecology* 25:509–518.
- McAdoo, B. G., D. L. Orange, E. A. Silver, K. McIntosh, L. Abbott, J. Galewsky, L. Kahn, and M. Protti.

1996. Seafloor structural observations, Costa Rica accretionary prism. *Geophysical Research Letters* 23:883–886.
- Mengerink, K. J., et al. 2014. A call for Deep-Ocean Stewardship. *Science* 344:696–698.
- Niemann, H., et al. 2013. Methane- carbon flow into the benthic food web at cold seeps: a case study from the Costa Rica subduction zone. *PLOS ONE* 8:e74894.
- NOAA. 2020. Amendment 28 to the Pacific coast groundfish fishery management plan. Federal Register 84:63966–63992.
- Orphan, V. J., C. H. House, K. U. Hinrichs, K. D. McKeegan, and E. F. DeLong. 2002. Multiple archaeal groups mediate methane oxidation in anoxic cold seep sediments. *Proceedings of the National Academy of Sciences of the United States of America* 99:7663–7668.
- Paul, B. G., H. Ding, S. C. Bagby, M. Y. Kellermann, M. C. Redmond, G. L. Andersen, and D. L. Valentine. 2017. Methane-oxidizing bacteria shunt carbon to microbial mats at a marine hydrocarbon seep. *Frontiers in Microbiology* 8:186.
- R Core Team. 2016. R: a language and environment for statistical computing. R Foundation for Statistical Computing, Vienna, Austria.
- Ramirez-Llodra, E., et al. 2011. Man and the last great wilderness: human impact on the deep sea. *PLOS ONE* 6:e22588.
- Reeburg, W. S. 2007. Oceanic methane biogeochemistry. *Chemical Reviews* 107:486–513.
- Riekenberg, P. M., R. S. Carney, and B. Fry. 2016. Trophic plasticity of the methanotrophic mussel *Bathymodiolus childressi* in the Gulf of Mexico. *Marine Ecology Progress Series* 547:91–106.
- Ritt, B., J. Sarrazin, J.-C. Caprais, P. Noël, O. Gauthier, C. Pierre, P. Henry, and D. Desbruyères. 2010. First insights into the structure and environmental setting of cold-seep communities in the Marmara Sea. *Deep-Sea Research Part I* 57:1120–1136.
- Rowden, A. A., D. Leduc, M. R. Clark, and D. A. Bowden. 2016. Habitat differences in deep-sea megafaunal communities off New Zealand: implications for vulnerability to anthropogenic disturbance and management. *Frontiers in Marine Science* 3:241.
- Sahling, H., D. G. Masson, C. R. Ranero, V. Hühnerbach, W. Weinrebe, I. Klauke, D. Bürk, W. Brückmann, and E. Suess. 2008. Fluid seepage at the continental margin offshore Costa Rica and southern Nicaragua. *Geochemistry, Geophysics, Geosystems* 9:Q05S05.
- Seabrook, S., F. C. De Leo, and A. R. Thurber. 2019. Flipping for food: the use of a methane seep by Tanner crabs (*Chionoecetes tanneri*). *Frontiers in Marine Science* 6:43.
- Shank, T. M., D. J. Fornari, K. L. Von Damm, M. D. Lilley, R. M. Haymon, and R. A. Lutz. 1998. Temporal and spatial patterns of biological community development at nascent deep-sea hydrothermal vents (9°50'N, East Pacific Rise). *Deep-Sea Research Part II* 45:465–515.
- Thiel, M. 1999. Duration of extended parental care in marine amphipods. *Journal of Crustacean Biology* 19:60–71.
- Thurber, A. R. 2014. Diet-dependent incorporation of biomarkers: implications for food-web studies using stable isotope and fatty acid analyses with special application to chemosynthetic environments. *Marine Ecology* 36:1–17.
- Thurber, A. R., L. A. Levin, V. J. Orphan, and J. J. Marlow. 2012. Archaea in metazoan diets: implications for food webs and biogeochemical cycling. *ISME Journal* 6:1602–1612.
- Tryon, M. D., K. M. Brown, M. E. Torres, A. M. Tréhu, J. McManus, and R. W. Collier. 1999. Measurements of transience and downward fluid flow near episodic methane gas vents, Hydrate Ridge, Cascadia. *Geology* 27:1075–1078.
- Tunncliffe, V., R. W. Embley, J. F. Holden, D. A. Butterfield, G. J. Massoth, and S. K. Juniper. 1997. Biological colonization of new hydrothermal vents following eruption on Juan de Fuca Ridge. *Deep-Sea Research Part I* 44(9–10):1627–1644.
- Tunncliffe, V., S. K. Juniper, and M. Sibuet. 2003. Reducing environments of the deep-sea floor. Pages 81–110 in *Ecosystems of the deep oceans*. Elsevier Science, Amsterdam.
- Turner, P. J., et al. 2020. Methane seeps on the US Atlantic margin and their potential importance to populations of the commercially valuable deep-sea red crab, *Chaceon quinque-dens*. *Frontiers in Marine Science* 7:75.
- Van Dover, C. L., C. R. Smith, J. Ardron, D. Dunn, K. Gjerde, L. Levin, S. Smith, and T. D. W. Contributors. 2012. Designating networks of chemosynthetic ecosystem reserves in the deep sea. *Marine Policy* 36:378–381.
- Vander Zanden, M. J., M. K. Clayton, E. K. Moody, C. T. Solomon, and B. C. Widel. 2015. Stable isotope turnover and half-life in animal tissues: a literature synthesis. *PLOS ONE* 10:e0116182.
- Vinn, O., K. Hryniewicz, C. T. S. Little, and H. A. Nakrem. 2014. A Boreal serpulid fauna from Volgian-Ryazanian (latest Jurassic-earliest Cretaceous) shelf sediments and hydrocarbon seeps from Svalbard. *Geodiversitas* 36:527–540.
- Vinn, O., E. K. Kupriyanova, and S. Kiel. 2013. Serpulids (Annelida, Polychaeta) at Cretaceous to modern hydrocarbon seeps: ecological and

- evolutionary patterns. *Palaeogeography, Palaeoclimatology, Palaeoecology* 390:35–41.
- Wiklund, W., A. G. Glover, P. J. Johannessen, and T. G. Dahlgren. 2009. Cryptic speciation at organic-rich marine habitats: a new bacteriovore annelid from whale-fall and fish farms in the north-east Atlantic. *Zoological Journal of the Linnean Society* 155:774–785.
- Xie, S., T. H. Dixon, R. Malservisi, Y. Jiang, M. Protti, and C. Muller. 2020. Slow slip and inter-transient locking on the Nicoya megathrust in the late and early stages of an Earthquake Cycle. *Journal of Geophysical Research: Solid Earth* 123: e2020JB020503.
- Zapata-Hernández, G., J. Sellanes, A. R. Thurber, L. A. Levin, F. Chazalon, and P. Linke. 2014. New insights on the trophic ecology of bathyal communities from the methane seep area off Concepción Chile (~36°S). *Marine Ecology* 35:1–21.

SUPPORTING INFORMATION

Additional Supporting Information may be found online at: <http://onlinelibrary.wiley.com/doi/10.1002/ecs2.3744>/full